Sliding-Mode Flux Observer With Online Rotor Parameter Estimation for Induction Motors

Amuliu Bogdan Proca, *Member, IEEE*, and Ali Keyhani, *Fellow, IEEE*

***Abstract*—Field orientation techniques without flux measurements depend on the parameters of the motor, particularly on the rotor resistance or rotor time constant (for rotor field orientation). Since these parameters change continuously as a function of temperature, it is important that the value of rotor resistance is continuously estimated online. A fourth-order sliding-mode flux observer is developed in this paper. Two sliding surfaces representing combinations of estimated flux and current errors are used to enforce the flux and current estimates to their real values. Switching functions are used to drive the sliding surfaces to zero. The equivalent values of the switching functions (low-frequency components) are proven to be the rotor resistance and the inverse of the rotor time constant. This property is used to simultaneously estimate the rotor resistance and the inverse of the time constant without prior knowledge of either the rotor resistance or the magnetizing inductance. Simulations and experimental results prove the validity of the proposed approach.**

***Index Terms*—Field-oriented control, induction motor, online parameter estimation, sliding mode.**

I. Introduction

In HIGH-PERFORMANCE applications, the induction motor is controlled through stator and rotor field-orientation techniques. Field orientation techniques are based on the knowledge of rotor (or stator) fluxes, and these fluxes are not measurable in practical applications. There are two common methods of rotor field orientation. The direct field orientation uses a flux observer for field orientation, whereas the indirect field orientation method uses the slip equation to calculate field orientation. Both methods depend on the parameters of the motor, particularly on the rotor resistance and magnetizing inductance. While the magnetizing inductance can be considered constant if the flux level is kept constant and can be easily mapped to the flux level by a saturation function if flux is variable, the rotor resistance varies as a function of skin effect and rotor temperature. The later is unmeasurable in practical conditions. It is therefore important for field orientation that the value of rotor resistance is continuously estimated online.

Extensive research has been performed on the topic by Sul [1], Toliyat *et al.* [2], Kubota and Matsuse [3], Marino *et al.* [4], [21]–[22], Zai *et al.* [5], and others [6]–[20]. Direct calculation methods compute rotor resistance values algebraically [1], [2], [6], [8]. In [1], the rotor resistance is computed directly from motor equations at steady-state conditions. In [2], the induced voltage in a phase [of a modified pulsewidth-modulated (PWM) inverter] is used to calculate the rotor resistance. In [6], the rotor resistance is calculated algebraically, provided that there is a flux and speed transient. In [8], Stephan *et al.* eliminate the flux terms from the motor equations and use a least squares algorithm to estimate the new system parameters. In [3] and [11]–[13], signal injection methods are used, whereas in [14], magnetic saliency properties are employed to estimate rotor parameters. Model reference adaptive systems were used in [9] and [15]–[17] to estimate the rotor resistance or the rotor time constant. The authors of [5] and [18]–[20] use an extended Kalman filter for the estimation of both fluxes and parameters. In [4], [10], [21], and [22], a nonlinear adaptive observer is used to simultaneously estimate fluxes and parameters.

More recently, sliding-mode observers and controllers were introduced for induction motor observers and controllers due to their intrinsic robustness to load and parameter uncertainties [24]–[29]. Utkin *et al.* have developed theoretical foundations for the sliding-mode control of induction motors [24]. In [25], Benchaib *et al.* build upon the concepts developed in [24] and present a practical implementation of the induction motor sliding-mode observer. In [26] and [27], adaptive sliding-mode observers are developed to estimate rotor flux and speed. In [28], Rehman *et al.* develop a sliding-mode flux and speed observer for the induction motor based on the current model. The observer is further improved by Derdiyok [29], who used a continuous-mode approach to eliminate the pure integration problem shown in [28].

The observer proposed in this paper is based on the induction motor model in stationary reference frame. It is a fourth-order sliding-mode observer and is used for both flux and parameter estimation. Two sliding surfaces representing the stator current amplitude and a combination of estimated flux and current errors are used to enforce the flux and current estimates to their real values. The observer does not depend on the values of the rotor resistance and rotor time constant. Employing the use of Lyapunov functions, it is proven that the sliding surfaces can be forced to zero in finite time by using two switching functions. Furthermore, the equivalent values of the switching functions (low-frequency components) are proven to be the rotor resistance and the inverse of the rotor time constant. This property is used to simultaneously estimate the rotor resistance and the inverse of the time constant without prior knowledge of either the rotor resistance or the magnetizing inductance. Furthermore, since the algorithm is quite robust to the variation

Manuscript received November 7, 2006; revised October 2, 2006. Abstract published on the Internet January 14, 2007.

A. B. Proca is with Ametek Solidstate Controls, Columbus, OH 43085 USA (e-mail: aproca@yahoo.com).

A. Keyhani is with the Department of Electrical Engineering, The Ohio State University, Columbus, OH 43210 USA (e-mail: keyhani.1@osu.edu).

Color versions of one or more of the figures in this paper are available online at http://ieeexplore.ieee.org.

Digital Object Identifier 10.1109/TIE.2007.891786

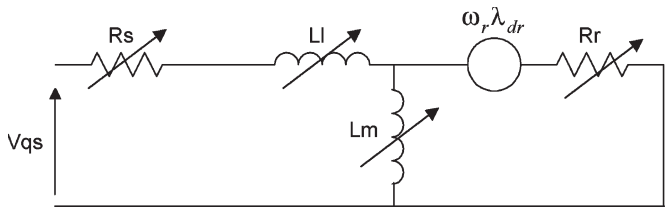

Fig. 1. Induction motor model in stationary reference frame (q-axis).

of leakage inductance, the only offline (or self-commissioned) estimation needed is for stator resistance.

II. Induction Motor Model

In this paper, we will use the induction motor model in the stationary reference frame, as shown in Fig. 1 for q-axis (d-axis is similar). As noted in [23], the model is equivalent (without any loss of information) to the more common T-model, in which the leakage inductance is separated in stator and rotor leakage.

The following equations for the induction machine can be derived:

$$\frac{di_{qs}}{dt} = \beta(-n_p\omega_r\lambda_{dr} + \eta\lambda_{qr} - R_s i_{qs} + v_{qs} - R_r i_{qs}) \quad (1)$$

$$\frac{di_{ds}}{dt} = \beta(n_p\omega_r\lambda_{qr} + \eta\lambda_{dr} - R_s i_{ds} + v_{ds} - R_r i_{ds}) \quad (2)$$

$$\frac{d\lambda_{qr}}{dt} = n_p\omega_r\lambda_{dr} - \eta\lambda_{qr} + R_r i_{qs} \quad (3)$$

$$\frac{d\lambda_{dr}}{dt} = -n_p\omega_r\lambda_{qr} - \eta\lambda_{dr} + R_r i_{ds} \quad (4)$$

where

v_{ds}, v_{qs}	stator voltages;
i_{ds}, i_{qs}	stator currents;
λ_{dr}, λ_{qr}	rotor fluxes, all in stationary reference frame;
n_p	number of poles pairs;
ω_r	rotor speed;
R_s, R_r	stator and rotor resistances;
η	$= R_r/L_m$;
β	$= 1/L_l$;

where L_m and L_l are the magnetizing and leakage inductances, respectively.

The electromagnetic torque expressed in terms of the state variables is

$$T_e = 3n_p(\lambda_{dr} i_{qs} - \lambda_{qr} i_{ds}). \quad (5)$$

III. Effect of Variation of Rotor Resistance on Field Orientation

Field (stator, rotor, or air gap) orientation methods need flux information to calculate the orientation angle. The rotor flux can be measured using flux sensors in the d–q axis positions; however, these sensors are costly and reduce the overall reliability of the system. A preferred method in the absence of flux measurements is the use of model-based field-oriented controllers. In this case, the variation of rotor resistance impacts the field orientation. Direct field-oriented controllers use the flux equations in stationary reference frame (3), (4) to calculate the orientation angle. Indirect field-oriented controllers use the slip equation for the same purpose, i.e.,

$$\frac{d\lambda_r}{dt} = -\eta \cdot \lambda_r^e + R_r \cdot i_{ds}^e \quad (6)$$

$$\frac{d\theta_e}{dt} = n_p\omega_r + R_r\frac{i_{qs}^e}{\lambda_r} \quad (7)$$

where

i_{ds}^e, i_{qs}^e	stator currents in synchronous reference frame;
λ_r	rotor flux in synchronous reference frame;
θ_e	orientation angle.

Both methods depend on the rotor parameters (η, R_r). Since rotor resistance varies as a function of temperature and skin effect, both rotor parameters will be affected, and errors in the values of these parameters will imply errors in field orientation [1]–[22]. An error in field orientation will result in an error in both the values of the tracked flux and of the tracked torque (assuming that the controllers are well tuned). The effects of the unaccounted for variation of rotor resistance on the values of flux and torque were analyzed through simulation, using the rated parameters of the motor employed in this paper. The results are not presented to make the length of the paper short. Although tracking errors were observed throughout the entire range of speed and loading, a higher tracking error in torque and flux will appear at higher loads since the sensitivity of the stator currents (and, consequently, torque and flux) to rotor resistance increases with loading. At high load, the error for both flux and torque is comparable in magnitude with the rotor resistance error.

IV. Sliding-Mode Observer Design

The sliding-mode flux observer is developed based on the motor dynamic equations

$$\frac{d\hat{i}_{qs}}{dt} = \beta(-n_p\omega_r\hat{\lambda}_{dr} + \hat{\eta}\hat{\lambda}_{qr} - R_s\hat{i}_{qs} + v_{qs} - \hat{R}_r\hat{i}_{qs}) \quad (8)$$

$$\frac{d\hat{i}_{ds}}{dt} = \beta(n_p\omega_r\hat{\lambda}_{qr} + \hat{\eta}\hat{\lambda}_{dr} - R_s\hat{i}_{ds} + v_{ds} - \hat{R}_r\hat{i}_{ds}) \quad (9)$$

$$\frac{d\hat{\lambda}_{qr}}{dt} = n_p\omega_r\hat{\lambda}_{dr} - \hat{\eta}\hat{\lambda}_{qr} + \hat{R}_r\hat{i}_{qs} \quad (10)$$

$$\frac{d\hat{\lambda}_{dr}}{dt} = -n_p\omega_r\hat{\lambda}_{qr} - \hat{\eta}\hat{\lambda}_{dr} + \hat{R}_r\hat{i}_{ds} \quad (11)$$

where the symbol $\hat{}$ represents estimated values.

The fourth-order observer appears similar in structure with a full-order open-loop observer. The difference consists in the terms $\hat{R}_r$ and $\hat{\eta}$ (replacing the parameters R_r and η), which are switching functions used to assure the convergence of the observer.

Define two sliding surfaces as

$$s_1 = i_{qs}^2 - \hat{i}_{qs}^2 + i_{ds}^2 - \hat{i}_{ds}^2 \quad (12)$$

$$s_2 = (i_{qs} - \hat{i}_{qs})\hat{\lambda}_{qr} + (i_{ds} - \hat{i}_{ds})\hat{\lambda}_{dr}. \quad (13)$$

Let a Lyapunov function (positive definite) be

$$V = 0.5 \cdot s^T s, \quad \text{where} \quad s = \begin{bmatrix} s_1 \\ s_2 \end{bmatrix}. \tag{14}$$

To prove the existence of a sliding mode, we are interested in finding the condition for which

$$\dot{V} = \dot{s}_1 \cdot s_1 + \dot{s}_2 \cdot s_2 < 0. \tag{15}$$

After some algebraic derivation, the derivative of s is

$$\dot{s} = \begin{bmatrix} f_1 \\ f_2 \end{bmatrix} + G \cdot \begin{bmatrix} \hat{R}_r \\ \hat{\eta} \end{bmatrix} \tag{16}$$

where f_1, f_2, and G are shown at the bottom of the page. The symbol Δ represents the estimation error, the difference between real and estimated values. Let

$$\begin{aligned} \begin{bmatrix} \hat{R}_r \\ \hat{\eta} \end{bmatrix} &= -\begin{bmatrix} K_r & 0 \\ 0 & K_\eta \end{bmatrix} \text{sign}(G^T s) \\ &= -\begin{bmatrix} K_r \cdot \text{sign}(g_1 s_1 + g_3 s_2) \\ K_\eta \cdot \text{sign}(g_2 s_1 + g_4 s_2) \end{bmatrix}. \end{aligned} \tag{17}$$

The Lyapunov function derivative becomes

$$\begin{aligned} \dot{V} = f_1 s_1 + f_2 s_2 - K_r \cdot (g_1 s_1 + g_3 s_2) \cdot \text{sign}(g_1 s_1 + g_3 s_2) \\ - K_\eta \cdot (g_2 s_1 + g_4 s_2) \cdot \text{sign}(g_2 s_1 + g_4 s_2). \end{aligned} \tag{18}$$

If K_r and K_η are positive constants chosen so that

$$K_r \cdot |g_1 s_1 + g_3 s_2| + K_\eta \cdot |g_2 s_1 + g_4 s_2| > |f_1 s_1 + f_2 s_2| \tag{19}$$

then the Lyapunov function derivative is negative, and s_1 and s_2 will converge to zero in a finite time, implying that the current estimates $(\hat{i}_{ds}, \hat{i}_{qs})$ will converge to their real values in a finite time.

The choice of switching functions is not unique. Due to the fact that, generally, $|g_1 s_1| > |g_3 s_2|$, $|g_4 s_2| > |g_2 s_1|$, $g_1 > 0$ while g_2 can be made negative by choosing initial values for the current close to the real values, the switching functions can be simplified to the form

$$\begin{bmatrix} \hat{R}_r \\ \hat{\eta} \end{bmatrix} = \begin{bmatrix} -K_r \cdot \text{sign}(s_1) \\ K_\eta \cdot \text{sign}(s_2) \end{bmatrix}. \tag{20}$$

This choice of switching functions is easier to compute (no need to compute matrix G), and it allows the decoupling of the sliding surfaces; it was therefore preferred in this paper.

Both $\hat{R}_r$ and $\hat{\eta}$ are switching functions containing a high-order harmonics. The equivalent values of $\hat{R}_r$ and $\hat{\eta}$ (the smoothed estimates $\hat{R}_{r,\text{eq}}$ and $\hat{\eta}_{\text{eq}}$) can be found by solving the equation $\dot{s} = 0$, $s = 0$ [24, Sec. 2.3]. Their derivation and a proof that the equivalent values are identical to R_r and η are presented in the Appendix. The analytical solution of $\hat{R}_{r,\text{eq}}$ and $\hat{\eta}_{\text{eq}}$ will contain unknown terms (R_r, η, λ_{dr}, and λ_{qr}) and therefore can only be used for demonstration purposes. A low-pass filter is used instead to extract the equivalent values [24], i.e.,

$$\hat{R}_{r,\text{eq}} = \frac{1}{1 + s \cdot \tau} \hat{R}_r \tag{21}$$

$$\hat{\eta}_{\text{eq}} = \frac{1}{1 + s \cdot \tau} \hat{\eta}. \tag{22}$$

The values of $\hat{R}_{r,\text{eq}}$ and $\hat{\eta}_{\text{eq}}$ will be used as estimates of R_r and η in the analysis of the observer.

V. Simulation Results

A. Convergence of the Observer

Extensive simulations were run to verify the convergence of the observer. The model used in the simulations has the same parameters as the one used in the experiments; these parameters are shown in tabular form in the Appendix.

Table I summarizes the estimation errors for R_r and η and the subsequent tracking of flux and torque at steady state. Since errors in the observer yield errors in field orientation, the errors in rotor flux estimation (in synchronous reference frame) and torque are also shown. As expected, larger parameter estimation errors can be expected in the low-load–high-speed region. However, flux estimation errors are small since the observer is least sensitive to rotor parameters in that region.

B. Robustness to Parameter Variation

Two of the model parameters, i.e., R_r and η, are estimated online using the presented observers, whereas R_s and L_l are not estimated online. The effect of the variation of R_s and L_l over the estimation of R_r and η and their impact on field orientation are shown in Tables II and III.

$$\begin{aligned} f_1 =& -R_r\beta\left(i_{qs}^2 + i_{ds}^2\right) - R_s\beta\left(i_{qs}^2 + i_{ds}^2 - \hat{i}_{qs}^2 - \hat{i}_{ds}^2\right) + \eta\beta(\lambda_{qr} i_{qs} + \lambda_{dr} i_{ds}) \\ & - \beta n_p \omega_r \left(\lambda_{qr} i_{ds} - \lambda_{dr} i_{qs} - \hat{\lambda}_{qr}\hat{i}_{ds} + \hat{\lambda}_{dr}\hat{i}_{qs}\right) + \beta v_{ds}\Delta i_{ds} + \beta v_{qs}\Delta i_{qs} \\ f_2 =& \, n_p\omega_r\left(\hat{\lambda}_{qr}\Delta i_{ds} - \hat{\lambda}_{dr}\Delta i_{qs}\right) - \beta n_p\omega_r\left(\hat{\lambda}_{qr}\Delta\lambda_{ds} - \hat{\lambda}_{dr}\Delta\lambda_{qs}\right) - R_r\beta(\hat{\lambda}_{qr} i_{qs} + \hat{\lambda}_{dr} i_{ds}) \\ & + \beta\eta(\lambda_{qr}\hat{\lambda}_{qr} + \lambda_{dr}\hat{\lambda}_{dr}) - R_s\beta\left(\hat{\lambda}_{qr}\Delta i_{qs} + \hat{\lambda}_{dr}\Delta i_{ds}\right) \\ G = \begin{bmatrix} g_1 & g_2 \\ g_3 & g_4 \end{bmatrix} =& \begin{bmatrix} \beta\left(\hat{i}_{qs}^2 + \hat{i}_{ds}^2\right) & -\beta\left(\hat{\lambda}_{dr}\hat{i}_{ds} + \hat{\lambda}_{qr}\hat{i}_{qs}\right) \\ \hat{i}_{ds}\Delta i_{ds} + \hat{i}_{qs}\Delta i_{qs} + \beta\left(\hat{\lambda}_{dr}\hat{i}_{ds} + \hat{\lambda}_{qr}\hat{i}_{qs}\right) & -\beta(\hat{\lambda}_{dr}^2 + \hat{\lambda}_{qr}^2) - \hat{\lambda}_{dr}\Delta i_{ds} - \hat{\lambda}_{qr}\Delta i_{qs} \end{bmatrix} \end{aligned}$$

TABLE I
CONVERGENCE OF THE PROPOSED OBSERVER FOR DIFFERENT VALUES OF SPEED AND LOAD

Speed (rpm)	100	1000	2000	100	1000	2000	100	1000	2000
Load(i^e_{qs} in amps)	2	2	2	8	8	8	15	15	15
Δ Rr(%)	4.73	6.00	15.25	0.98	0.55	1.19	1.10	0.19	0.49
$\Delta \eta$(%)	5.59	7.44	17.53	1.33	0.66	0.52	0.34	-1.51	-3.20
$\Delta \lambda$(%)	0.53	0.29	0.61	-0.16	0.36	0.73	0.54	0.37	0.68
Δ T(%)	0.03	0.30	0.60	0.38	0.71	1.29	0.83	0.62	1.08

TABLE II
EFFECT OF UNCERTAINTY OF STATOR RESISTANCE ON OBSERVER

Speed (rpm)		100	1000	2000	100	1000	2000	100	1000	2000
Load(i^e_{qs} in amps)		2	2	2	8	8	8	15	15	15
Δ Rs=-75%	Δ Rr(%)	29.32	11.97	35.97	-15.23	0.42	8.30	-39.35	-5.06	-1.46
	$\Delta \eta$(%)	37.23	15.55	38.48	30.55	15.12	34.20	34.07	12.38	23.49
	$\Delta \lambda$(%)	-11.79	-0.60	0.13	-38.56	-3.28	-1.38	-52.17	-6.17	-3.31
	Δ T(%)	-49.85	-4.03	-2.24	-43.33	-3.80	-1.40	-51.97	-6.37	-3.17
Δ Rs=-50%	Δ Rr(%)	14.82	7.33	16.47	-9.98	-0.19	1.66	-25.98	-3.40	-1.56
	$\Delta \eta$(%)	25.96	9.80	19.29	21.53	6.32	8.95	24.74	4.89	3.93
	$\Delta \lambda$(%)	-7.43	-0.30	0.27	-25.78	-1.99	-0.74	-34.31	-3.93	-2.01
	Δ T(%)	-32.13	-2.63	-1.21	-29.22	-2.22	-0.56	-34.26	-3.99	-1.81
Δ Rs=-25%	Δ Rr(%)	11.02	6.66	15.89	-4.65	0.12	1.11	-12.31	-1.60	-0.59
	$\Delta \eta$(%)	16.96	8.61	18.42	12.59	3.14	3.23	13.69	1.51	-0.58
	$\Delta \lambda$(%)	-3.22	-0.01	0.44	-13.08	-0.80	0.02	-16.75	-1.79	-0.64
	Δ T(%)	-15.78	-1.16	-0.31	-14.74	-0.75	0.39	-16.58	-1.69	-0.34
Δ Rs=25%	Δ Rr(%)	-1.91	5.36	14.74	8.58	1.03	1.64	15.60	1.97	1.62
	$\Delta \eta$(%)	-7.32	6.28	16.69	-11.88	-1.31	-0.56	-17.35	-4.31	-5.16
	$\Delta \lambda$(%)	4.12	0.58	0.78	11.29	1.50	1.42	17.02	2.48	1.97
	Δ T(%)	16.09	1.76	1.49	13.91	2.15	2.17	18.22	2.89	2.48
Δ Rs=50%	Δ Rr(%)	-8.33	4.70	14.12	16.45	1.84	2.12	31.02	3.78	2.78
	$\Delta \eta$(%)	-20.95	5.09	15.78	-27.14	-2.75	-1.43	-37.05	-6.78	-6.63
	$\Delta \lambda$(%)	7.75	0.87	0.95	21.58	2.63	2.10	33.43	4.55	3.24
	Δ T(%)	31.74	3.23	2.40	26.93	3.57	3.03	35.73	5.12	3.85
Δ Rs=75%	Δ Rr(%)	-13.25	4.03	13.53	24.97	2.68	2.61	47.56	5.69	3.94
	$\Delta \eta$(%)	-33.96	3.90	14.90	-42.59	-4.19	-2.31	-44.26	-9.20	-8.11
	$\Delta \lambda$(%)	11.70	1.16	1.11	32.09	3.76	2.78	49.86	6.63	4.51
	Δ T(%)	47.04	4.69	3.30	39.89	5.00	3.90	52.49	7.37	5.22

It can be seen that the effect of uncertainties of the leakage inductance on flux and torque estimation is minimal even for large uncertainties ($\pm$75%). Furthermore, the leakage inductance can be easily mapped to the stator current amplitude as a saturation function. The effect of stator resistance uncertainties is not negligible, especially in the low-speed range. In situations in which the stator resistance varies considerably, a stator resistance observer is needed. In this paper, stator temperature was available from a temperature sensor. The stator resistance was mapped to stator temperature using a linear function.

VI. EXPERIMENTAL RESULTS

A. Experimental Setup

The experimental setup used in this paper is shown in Fig. 2. The induction motor (IM) has the following specifications: three phases, four poles, 5 hp, and 1750-r/min 220-V squirrel cage. The synchronous generator (S.G.) has the following specifications: two phases, two poles, 5 hp, and 440 V; it is used as a load. The 5-kW variable resistor box (R) loads the synchronous generator. A variable dc power supply controls the excitation of the synchronous generator. The motor is driven by a 400-V/30-A power converter capable of switching at 20 kHz. A dual-processor DSP board (TMS320C31 Master and TMS320P14 Slave) used both for control and data acquisition. A 1024-pulse/revolution incremental optical encoder is used for speed measurement. The PWM cycle is 240 μs, and the data acquisition sampling time is 60 μs. In order to avoid aliasing, the measured voltage is passed through a low-pass filter prior to being acquired. The synchronous generator can be controlled simultaneously with the motor using the DSP board through the excitation voltage.

TABLE III
EFFECT OF UNCERTAINTY OF LEAKAGE INDUCTANCE ON OBSERVER

Speed (rpm)		100	1000	2000	100	1000	2000	100	1000	2000
Load(i^e_{qs} in amps)		2	2	2	8	8	8	15	15	15
Δ Ll=-75%	Δ Rr(%)	-7.72	-3.66	32.37	-14.63	-15.26	-12.53	-18.45	-19.44	-17.69
	Δ η(%)	-0.33	4.66	40.63	-30.42	-29.99	-23.67	-93.81	-92.02	-80.21
	Δ λ(%)	-5.55	-6.29	-6.02	-6.05	-7.00	-6.76	-7.52	-9.15	-9.14
	Δ T(%)	2.14	0.85	1.12	1.79	1.03	1.57	1.86	0.95	1.30
Δ Ll=-50%	Δ Rr(%)	-3.29	-0.51	21.21	-8.78	-9.28	-7.82	-11.03	-11.88	-10.97
	Δ η(%)	1.20	4.76	26.97	-19.81	-20.32	-17.90	-63.88	-66.23	-61.54
	Δ λ(%)	-3.74	-4.10	-3.78	-4.61	-4.42	-4.13	-4.70	-5.45	-5.37
	Δ T(%)	0.66	0.61	0.88	0.48	0.86	1.43	1.02	0.79	1.16
Δ Ll=-25%	Δ Rr(%)	0.83	2.70	16.19	-3.69	-4.05	-3.22	-4.51	-5.17	-4.71
	Δ η(%)	3.33	5.92	20.11	-9.13	-9.80	-9.38	-31.69	-34.11	-34.39
	Δ λ(%)	-1.60	-1.90	-1.58	-2.52	-1.95	-1.62	-1.80	-2.25	-2.03
	Δ T(%)	0.26	0.45	0.74	0.11	0.77	1.36	0.84	0.67	1.12
Δ Ll=25%	Δ Rr(%)	8.52	9.52	16.26	5.38	4.45	5.25	6.53	4.09	4.34
	Δ η(%)	7.89	9.32	16.83	11.71	10.89	11.10	32.13	30.75	29.01
	Δ λ(%)	2.65	2.47	2.79	2.32	2.50	2.89	1.82	2.35	2.74
	Δ T(%)	-0.15	0.16	0.44	0.91	0.68	1.23	0.78	0.63	1.06
Δ Ll=50%	Δ Rr(%)	12.21	12.93	18.26	9.53	7.94	8.78	10.20	6.33	6.74
	Δ η(%)	10.22	11.21	17.21	22.10	21.33	21.39	62.93	63.02	61.12
	Δ λ(%)	4.77	4.64	4.96	4.55	4.45	4.86	1.50	3.68	4.14
	Δ T(%)	-0.28	0.05	0.28	1.36	0.66	1.19	-0.06	0.68	1.11
Δ Ll=75%	Δ Rr(%)	15.85	16.45	20.74	13.47	11.12	11.81	10.39	7.18	7.69
	Δ η(%)	12.59	13.33	18.19	32.50	31.99	31.70	92.67	95.63	93.80
	Δ λ(%)	6.87	6.79	7.12	6.45	6.19	6.63	3.17	4.31	4.78
	Δ T(%)	-0.37	-0.06	0.13	1.74	0.66	1.17	1.04	0.80	1.16

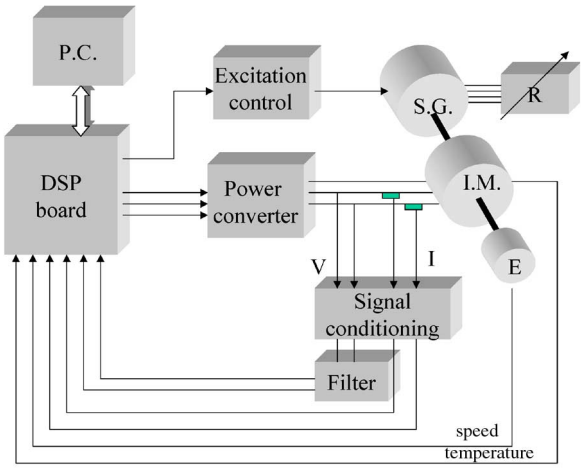

Fig. 2. Experimental setup.

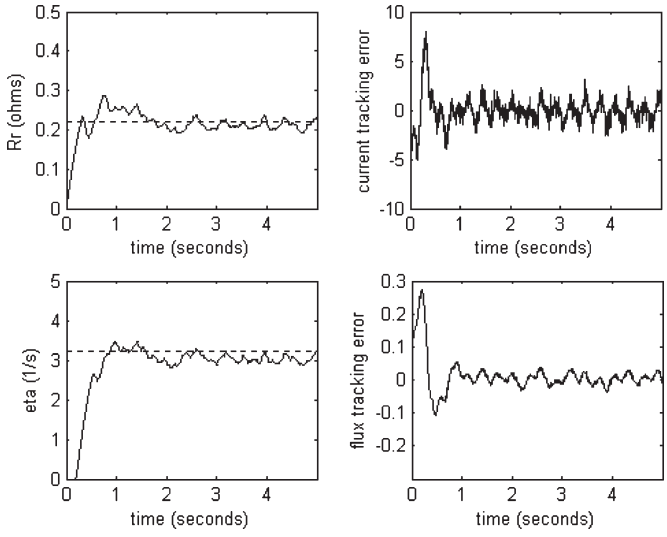

Fig. 3. Observer convergence for low speed/no load.

B. Observer Convergence

Extensive testing has been performed with the proposed observer. To show the convergence of the flux, observer tests were run at low speed (100 r/min), medium speed (1000 r/min), and high speed (2000 r/min). For each speed level, three loading conditions were considered: 1) no load; 2) medium load (8 N · m); and 3) high load (16 N · m). Figs. 3–6 are some examples of the results. The graphs on the right side are the current and flux errors (respectively) for the d-component (the q component is similar). The graphs on the left side represent the estimates of rotor resistance and time constant inverse; the dotted line represents the real value.

C. Load Step

Another set of tests consisted of a step in the motor load (Figs. 7 and 8). The top graphs show the behavior of the

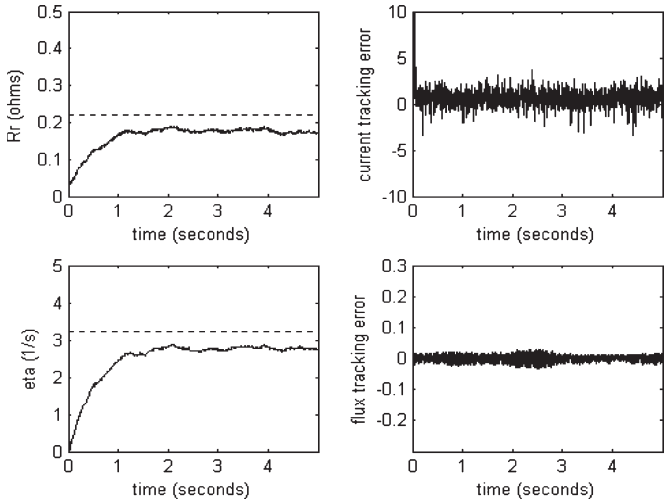

Fig. 4. Observer convergence for high speed/no load.

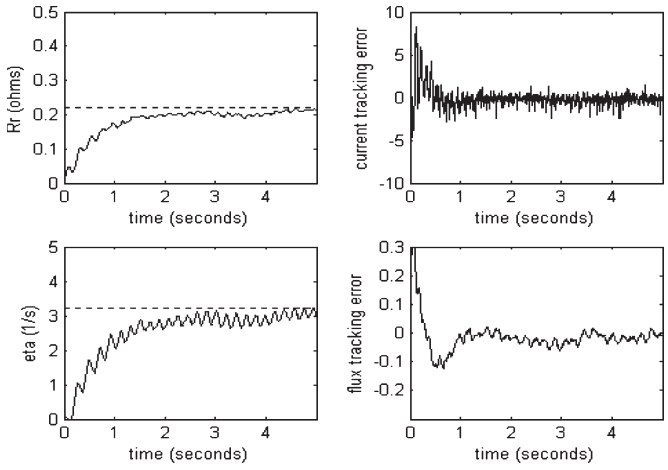

Fig. 5. Observer convergence for low speed/high load.

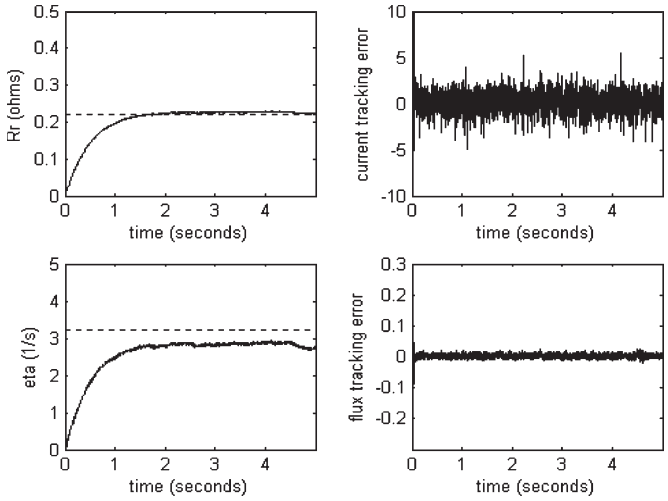

Fig. 6. Observer convergence for high speed/high load.

estimates of rotor resistance and inverse of time constant, whereas the bottom graphs show the torque current and speed, respectively.

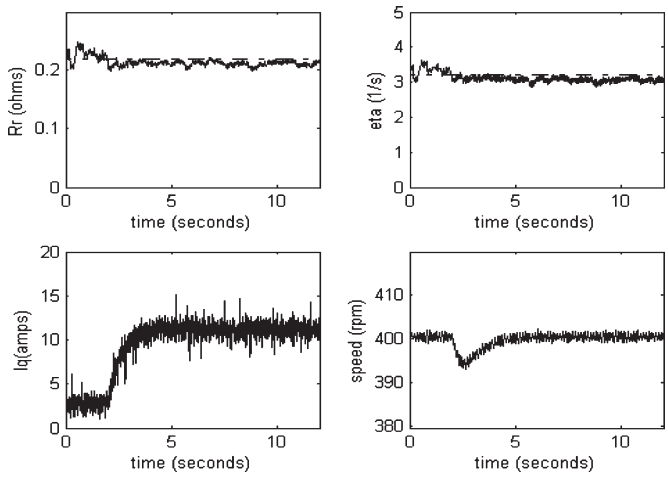

Fig. 7. Load step at 400 r/min.

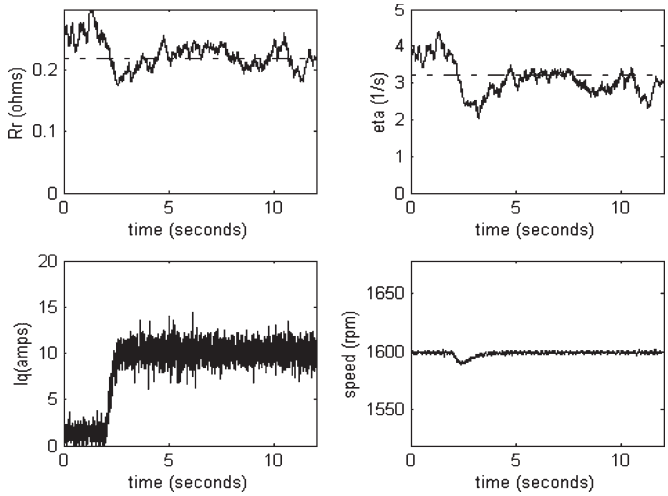

Fig. 8. Load step at 1600 r/min.

D. Tracking of a Variable Reference

To represent a continuously dynamic condition, the speed reference was made sinusoidal. The following graphs show the flux convergence and current convergence together with the estimates of rotor resistance and inverse of time constant (Fig. 9). The second plot shows the reference speed and measured speed.

VII. Conclusion

A sliding-mode flux observer was developed in this paper. The observer not only allows flux observation but also calculates the values of rotor resistance and the inverse of the rotor time constant. Due to the low sensitivity to rotor resistance of the stator currents, higher errors in the R_r and η are obtained when the motor operates at low levels of torque. However, due to the same sensitivity, the errors in flux and torque estimation are small. Furthermore, throughout the entire speed and load range, provided that the leakage inductance and stator resistance are known, the flux and torque estimation

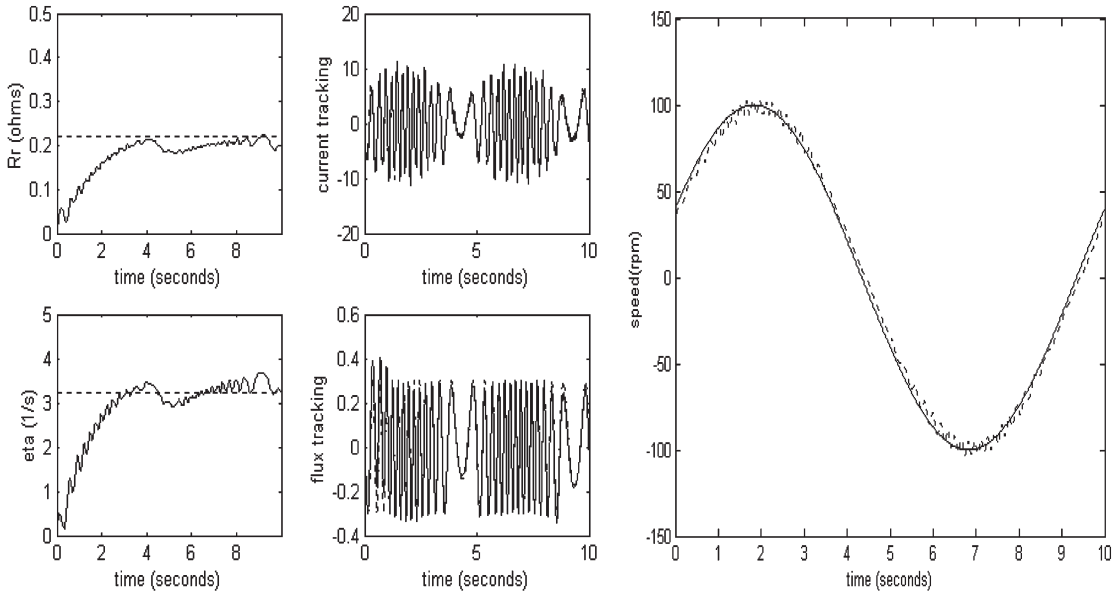

Fig. 9. Observer behavior for a sinusoidal speed reference.

errors are small (below 2%). The observer is robust to uncertainties in the leakage inductance values but relatively sensitive to uncertainties in the stator resistance values. Simulations and experimental results prove the validity of the current approach.

APPENDIX

TABLE IV
INDUCTION MOTOR RATED PARAMETERS

Rs	0.39 Ω
Ll	0.006 Henry
Lm	0.066 Henry
Rr	0.22 Ω

Equivalent Values

The equivalent values of $\hat{R}_r$ and $\hat{\eta}$ (the smoothed estimates $\hat{R}_{r,\mathrm{eq}}$ and $\hat{\eta}_{\mathrm{eq}}$) can be found by solving the equation $\dot{s} = 0$, $s = 0$. This yields

$$\hat{\eta}_{\mathrm{eq}} = \eta \frac{e_1}{\hat{e}_1} - \frac{i_s^2 R_r + v_{ds}\Delta i_{ds} + v_{qs}\Delta i_{qs} + n_p\omega_r\,(e_2 - \hat{e}_2)}{\hat{e}_1} - \frac{R_r\beta i_s^2(e_1^2 - \hat{\lambda}_r^2 i_s^2) + K i_s^2}{\hat{e}_1\left[-\hat{e}_1\left(\beta\hat{e}_1 + \hat{i}_{qs}\Delta i_{qs} + \hat{i}_{ds}\Delta i_{ds}\right) + \beta i_s^2\hat{\lambda}_r^2\right]} \tag{A1}$$

$$\hat{R}_{r,\mathrm{eq}} = \frac{R_r\beta\left(e_1^2 - \hat{\lambda}_r^2 i_s^2\right) + K}{\hat{e}_1\left(\beta\hat{e}_1 + \hat{i}_{qs}\Delta i_{qs} + \hat{i}_{ds}\Delta i_{ds}\right) - \beta i_s^2\hat{\lambda}_r^2} \tag{A2}$$

where

$$\begin{aligned} K = &-\hat{e}_1\Big[n_p\omega_r\left(-\hat{\lambda}_{dr}\Delta i_{qs} + \hat{\lambda}_{qr}\Delta i_{ds}\right) - \beta n_p\omega_r \\ &\times\left(\Delta\lambda_{qr}\hat{\lambda}_{dr} - \Delta\lambda_{dqr}\hat{\lambda}_{qr}\right) + \beta\eta(\lambda_{dr}\hat{\lambda}_{dr} + \lambda_{qr}\hat{\lambda}_{qr})\Big] \\ &+ \beta\hat{\lambda}_r^2\left[\eta e_1 + v_{ds}\Delta i_{ds} + v_{qs}\Delta i_{qs} + n_p\omega_r\,(e_2 - \hat{e}_2)\right] \\ e_1 = &\lambda_{dr} i_{ds} + \lambda_{qr} i_{qs}, \quad \hat{e}_1 = \hat{\lambda}_{dr}\hat{i}_{ds} + \hat{\lambda}_{qr}\hat{i}_{qs} \\ e_2 = &\lambda_{dr} i_{qs} - \lambda_{qr} i_{ds}, \quad \hat{e}_2 = \hat{\lambda}_{dr}\hat{i}_{qs} - \hat{\lambda}_{qr}\hat{i}_{ds} \\ \hat{\lambda}_r^2 = &\hat{\lambda}_{dr}^2 + \hat{\lambda}_{qr}^2, \quad i_s^2 = i_{ds}^2 + i_{qs}^2. \end{aligned}$$

If the flux and current estimates converge to their real values, then $\hat{e}_1 = e_1$, $\hat{e}_2 = e_2$, $K = 0$, and the equivalent values of $\hat{R}_r$ and $\hat{\eta}$ will converge to their real values, i.e.,

$$\hat{R}_{r,\mathrm{eq}} = R_r, \quad \hat{\eta}_{\mathrm{eq}} = \eta.$$

To prove the current and flux convergence, one needs to substitute the equations of $\hat{R}_{r,\mathrm{eq}}$ and $\hat{\eta}_{\mathrm{eq}}$ in the observer equations and prove that the estimates converge to their real values. At the time of writing this paper, the authors were not able to prove the convergence analytically. However, simulation and results for various speed and loading conditions show the validity of the concept.

ACKNOWLEDGMENT

The authors would like to thank V. I. Utkin of The Ohio State University for his help in performing this study.

REFERENCES

[1] S. K. Sul, "A novel technique of rotor resistance estimation considering variation of mutual inductance," *IEEE Trans. Ind. Appl.*, vol. 25, no. 4, pp. 578–587, Jul./Aug. 1989.

[2] H. A. Toliyat, M. S. Arefeen, K. M. Rahman, and D. Figoli, "Rotor time constant updating scheme for a rotor flux-oriented induction motor drive," *IEEE Trans. Power Electron.*, vol. 14, no. 5, pp. 850–857, Sep. 1999.

[3] H. Kubota and K. Matsuse, "Speed sensorless field-oriented control of induction motor with rotor resistance adaptation," *IEEE Trans. Ind. Appl.*, vol. 30, no. 5, pp. 1219–1224, Sep./Oct. 1994.
[4] R. Marino, S. Peresada, and P. Tomei, "On-line stator and rotor resistance estimation for induction motors," *IEEE Trans. Control Syst. Technol.*, vol. 8, no. 3, pp. 570–579, May 2000.
[5] L. C. Zai, C. L. De Marco, and T. A. Lipo, "An extended Kalman filter approach to rotor time constant measurement in PWM induction motor dries," *IEEE Trans. Ind. Appl.*, vol. 28, no. 1, pp. 96–104, Jan./Feb. 1992.
[6] K. Akatsu and A. Kawamura, "Online rotor resistance estimation using the transient state under the speed sensorless control of induction motor," *IEEE Trans. Power Electron.*, vol. 15, no. 3, pp. 553–560, May 2000.
[7] T. Saitoh, T. Okuyama, and T. Matsui, "An automated secondary resistance identification scheme in vector controlled induction motor drives," in *Conf. Rec. IEEE Ind. Appl. Soc. Annu. Meeting*, 1989, vol. 1, pp. 594–600.
[8] J. Stephan, M. Bodson, and J. Chiasson, "Real-time estimation of the parameters and fluxes of induction motors," *IEEE Trans. Ind. Appl.*, vol. 30, no. 3, pp. 746–759, May/Jun. 1994.
[9] R. D. Lorenz and D. B. Lawson, "A simplified approach to continuous on-line tuning of field-oriented induction machine drives," *IEEE Trans. Ind. Appl.*, vol. 26, no. 3, pp. 420–424, May/Jun. 1990.
[10] B. Aloliwi, H. K. Khalil, and E. G. Strangas, "Robust speed control of induction motors using adaptive observer," in *Proc. Amer. Control Conf.*, 1999, vol. 2, pp. 931–935.
[11] S. Wade, M. W. Dunnigan, and B. W. Williams, "New method of rotor resistance estimation for vector-controlled induction machines," *IEEE Trans. Ind. Electron.*, vol. 44, no. 2, pp. 247–257, Apr. 1997.
[12] M. Montanari, S. Peresada, A. Tilli, and A. Tonielli, "Speed sensorless control of induction motor based on indirect field-orientation," in *Conf. Rec. IEEE Ind. Appl. Soc. Annu. Meeting*, 2000, vol. 3, pp. 1858–1865.
[13] I.-J. Ha and S.-H. Lee, "An online identification method for both stator- and rotor resistances of induction motors without rotational transducers," *IEEE Trans. Ind. Electron.*, vol. 47, no. 4, pp. 842–853, Aug. 2000.
[14] K. D. Hurst, T. G. Habetler, G. Griva, F. Profumo, and P. L. Jansen, "A self-tuning closed-loop flux observer for sensorless torque control of standard induction machines," *IEEE Trans. Power Electron.*, vol. 12, no. 5, pp. 807–815, Sep. 1997.
[15] L. Zhen and L. Xu, "Sensorless field orientation control of induction machines based on a mutual MRAS scheme," *IEEE Trans. Ind. Electron.*, vol. 45, no. 5, pp. 824–831, Oct. 1998.
[16] M. S. N. Said and M. E. H. Benbouzid, "Induction motors direct field oriented control with robust on-line tuning of rotor resistance," *IEEE Trans. Energy Convers.*, vol. 14, no. 4, pp. 1038–1042, Dec. 1999.
[17] F.-J. Lin and H.-M. Su, "A high-performance induction motor drive with on-line rotor time-constant estimation," *IEEE Trans. Energy Convers.*, vol. 12, no. 4, pp. 297–303, Dec. 1997.
[18] L. Salvatore, S. Stasi, and L. Tarchioni, "A new EKF-based algorithm for flux estimation in induction machines," *IEEE Trans. Ind. Electron.*, vol. 40, no. 5, pp. 496–504, Oct. 1993.
[19] D. J. Atkinson, P. Acarnley, and J. W. Finch, "Observers for induction motor state and parameter estimation," *IEEE Trans. Ind. Appl.*, vol. 27, no. 6, pp. 1119–1127, Nov./Dec. 1991.
[20] M. S. N. Said, M. E. H. Benbouzid, and A. Benchaib, "Detection of broken bars in induction motors using an extended Kalman filter for rotor resistance sensorless estimation," *IEEE Trans. Energy Convers.*, vol. 15, no. 1, pp. 66–70, Mar. 2000.
[21] R. Marino, S. Peresada, and P. Tomei, "Global adaptive output feedback control of induction motors with uncertain rotor resistance," *IEEE Trans. Autom. Control*, vol. 44, no. 5, pp. 967–983, May 1999.
[22] ——, "Exponentially convergent rotor resistance estimation for induction motors," *IEEE Trans. Ind. Electron.*, vol. 42, no. 5, pp. 508–515, Oct. 1995.
[23] G. R. Slemon, "Modeling of induction machines for electric drives," *IEEE Trans. Ind. Appl.*, vol. 25, no. 6, pp. 1126–1131, Nov./Dec. 1989.
[24] V. Utkin, J. Guldner, and J. Shi, *Sliding Mode Control in Electromechanical Systems*. New York: Taylor & Francis, 1999.
[25] A. Benchaib, A. Rachid, E. Audrezet, and M. Tadjine, "Real-time sliding mode observer and control of an induction motor," *IEEE Trans. Ind. Electron.*, vol. 46, no. 1, pp. 128–138, Feb. 1999.
[26] Y. Zheng, H. A. A. Fattah, and K. A. Loparo, "Non-linear adaptive sliding mode observer-controller scheme for induction motors," *Int. J. Adapt. Control Signal Process.*, vol. 14, no. 2/3, pp. 245–273, Mar. 2000.
[27] M. Tursini, R. Petrella, and F. Parasiliti, "Adaptive sliding mode observer for speed sensorless control of induction motors," *IEEE Trans. Ind. Appl.*, vol. 36, no. 5, pp. 1380–1387, Sep./Oct. 2000.
[28] H. Rehman, A. Derdiyok, M. K. Guven, and L. Xu, "A new current model flux observer for wide speed range sensorless control of an induction machine," *IEEE Trans. Power Electron.*, vol. 17, no. 6, pp. 1041–1048, Nov. 2002.
[29] A. Derdiyok, "Speed-sensorless control of induction motor using a continuous control approach of sliding-mode and flux observer," *IEEE Trans. Ind. Electron.*, vol. 52, no. 4, pp. 1170–1176, Aug. 2005.

Amuliu Bogdan Proca (S'95–M'01) received the B.S. degree from the "Politehnica" University of Bucharest, Bucharest, Romania, in 1992, and the M.S.E.E. and Ph.D. degrees from The Ohio State University, Columbus, in 1997 and 2001, respectively.

He is currently with Ametek Solidstate Controls, Columbus. His research interests are in the areas of control of uninterruptible power supplies, distributed generation systems, electric motor drives, and power converters.

Ali Keyhani (S'72–M'76–SM'89–F'98) received the Ph.D. degree from Purdue University, West Lafayette, IN, in 1975.

He was with Hewlett-Packard Company and TRW Control, from 1967 to 1972. He is currently a Professor of electrical engineering at The Ohio State University (OSU), Columbus. He serves as the Director of the Electromechanical and Mechatronic Systems Laboratory, OSU. His research activities focus on the control of distributed energy systems, design and modeling of electric machine, control and design of power electronic systems, DSP-based virtual test bed for design, control of power systems, automotive systems, modeling, parameter estimation, and failure detection systems.

Dr. Keyhani was an Editor of the IEEE TRANSACTIONS ON ENERGY CONVERSION and is a past Chairman of the Electric Machinery Committee, IEEE Power Engineering Society. He received OSU College of Engineering Research Awards in 1989, 1999, and 2003.